54th Meeting of the APS Division of Plasma Physics, Providence, Rhode Island, October 2012

Numerical Simulations of NBI-driven CAE modes in H-mode Discharges in NSTX

E. V. Belova, N. N. Gorelenkov, N. A. Crocker,
E. D. Fredrickson

NSTX-U

PPPL
PRINCETON PLASMA PHYSICS LABORATORY

Abstract

Excitation of co- and counter-propagating compressional Alfven modes (CAEs) have been observed for H-mode NSTX discharges. Hybrid 3D code HYM has been used to investigate properties of beam ion driven CAE modes in NSTX. The HYM code is a nonlinear, global stability code in toroidal geometry, which includes fully kinetic ion description. Numerical simulations have been performed for the NSTX shots with strong CAE activity. It is shown that co-propagating CAE mode can be excited for large toroidal mode numbers $n \geq 8$ and frequency range $f > 0.4 f_{ci}$, consistent with observations. In contrast to GAE modes, large compressional magnetic perturbation is seen both in the core and at the plasma edge for CAE modes. Conditions which are favorable for CAE instability are studied, including the effects of the plasma density profiles, beam ion parameters, and magnetic profiles. It is shown that lower energy beam ions satisfy regular resonance conditions, whereas high energy beam ions satisfy Doppler-shifted cyclotron resonance condition.

Motivation

• Many sub-cyclotron frequency modes are observed in NSTX during NBI injection. These modes were identified as Compressional Alfven Eigenmodes (CAEs) and Global Alfven Eigenmodes (GAEs).

• CAE and GAE modes are predicted to be driven unstable by super Alfvenic NBI ions with $V_b \sim 3V_A$ (90 keV) through the Doppler shifted cyclotron resonance.

• GAE and CAE modes are capable of inducing redistribution of beam ions and strong anomalous electron transport in STs.

• Numerical simulations include: self-consistent anisotropic equilibrium, fully kinetic beam ion description and nonlinear effects.

HYM – Parallel Hybrid/MHD Code

HYM code developed at PPPL and used to investigate kinetic effects on MHD modes in toroidal geometry (FRCs and NSTX)

- 3-D nonlinear.
- Several different physical models:
  - Resistive MHD & Hall-MHD.
  - Hybrid (fluid electrons, particle ions).
  - MHD/particle (one-fluid thermal plasma, + energetic particle ions).
- Full-orbit kinetic ions.
- Drift-kinetic electrons.
- For particles: delta-f / full-f numerical scheme.
- Parallel (3D domain decomposition, MPI)[1].

[1]Simulations are performed at NERSC.

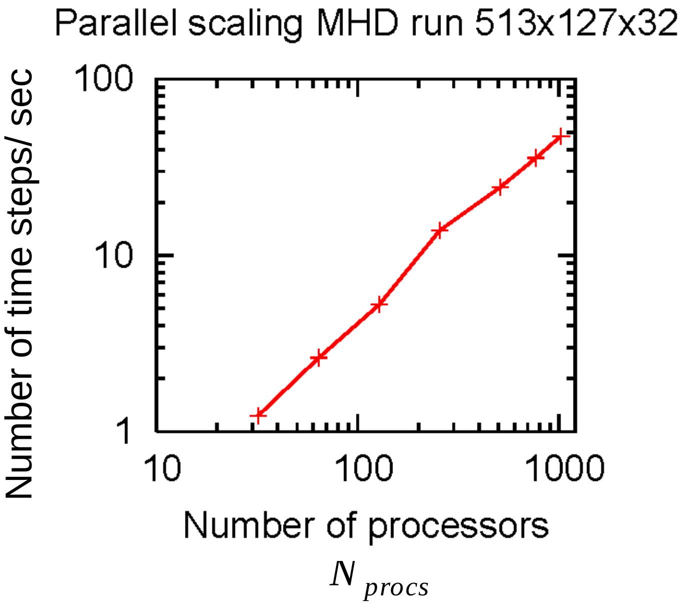

MPI version of HYM code shows very good parallel scaling up to 1000 processors for production-size simulation runs, and allows high-resolution nonlinear simulations.

Self-consistent MHD + fast ions coupling scheme

Background plasma - fluid:

$$\rho \frac{d\mathbf{V}}{dt} = -\nabla p + (\mathbf{j} - \mathbf{j}_i) \times \mathbf{B} - n_i (\mathbf{E} - \eta \mathbf{j})$$

$$\mathbf{E} = -\mathbf{V} \times \mathbf{B} + \eta \mathbf{j}$$

$$\mathbf{B} = \mathbf{B}_0 + \nabla \times \mathbf{A}$$

$$\partial \mathbf{A} / \partial t = -\mathbf{E}$$

$$\mathbf{j} = \nabla \times \mathbf{B}$$

$$\partial p^{1/\gamma} / \partial t = -\nabla \cdot (\mathbf{V} p^{1/\gamma})$$

$$\partial \rho / \partial t = -\nabla \cdot (\mathbf{V} \rho)$$

Fast ions – delta-F scheme:

$$\frac{d\mathbf{x}}{dt} = \mathbf{v}$$

$$\frac{d\mathbf{v}}{dt} = \mathbf{E} - \eta \mathbf{j} + \mathbf{v} \times \mathbf{B}$$

$w = \delta F / F$ - particle weight

$$\frac{dw}{dt} = -(1-w) \frac{d(\ln F_0)}{dt}$$

$$F_0 = F_0(\varepsilon, \mu, p_\phi)$$

ρ, **V** and p are bulk plasma density, velocity and pressure, n_i and $\boldsymbol{j}_i$ are fast ion density and current, $n_i << n$ – is assumed.

Self-consistent anisotropic equilibrium including the NBI ions

Grad-Shafranov equation for two-component plasma: MHD plasma (thermal) and fast ions [Belova et al, Phys. Plasmas 2003]

$$\frac{\partial^2\psi}{\partial z^2} + R\frac{\partial}{\partial R}\left(\frac{1}{R}\frac{\partial\psi}{\partial R}\right) = -R^2 p' - HH' - GH' + RJ_{i\phi}$$

$$\mathbf{B} = \nabla\phi\times\nabla\psi + h\nabla\phi$$

$$h(R,z) = H(\psi) + G(R,z)$$

$\mathbf{J}_{ip} = \nabla G\times\nabla\phi$, G – poloidal stream function

Fast ions – delta-f scheme: $F_0=F_0(\varepsilon,\mu,p_\varphi)$, where μ is calculated up to 1st order in ρ_i /L; F_0 is chosen to match the distribution functions computed from the TRANSP code (L-mode discharges).

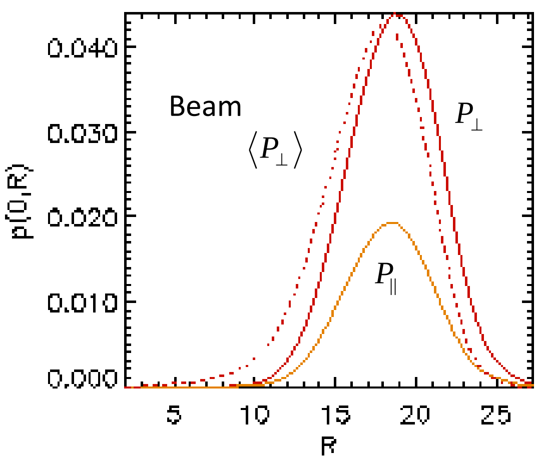

The prompt-loss condition, anisotropy, the large Larmor radius of the beam ions and the strong pitch-angle scattering at low energies have been included in order to match the distribution functions computed from the TRANSP code.

Strong modifications of equilibrium profiles due to beam ions: more peaked current profile, anisotropic pressure, increase in Shafranov shift – indirect effect on stability.

NSTX-U

PPPL PRINCETON PLASMA PHYSICS LABORATORY

Equilibrium calculations

Equilibrium distribution function $F_0 = F_1(v)F_2(\lambda)F_3(p_\phi)$

$$
\begin{aligned}
F_1(v) &= \frac{1}{v^3 + v_*^3}, \quad \text{for} \quad v < v_0 \\
F_2(\lambda) &= \exp(-(\lambda - \lambda_0)^2/\Delta\lambda^2) \\
F_3(p_\phi) &= \frac{(p_\phi - p_0)^\beta}{(R_0 v - \psi_0 - p_0)^\beta}, \quad \text{for} \quad p_\phi > p_0
\end{aligned}
$$

where $v_0 \approx 3v_A$, $\quad v_* = v_0/\sqrt{3}$, $\quad \lambda = \mu B_0/\varepsilon$ - pitch angle,
$\lambda_0 = 0.8 - 1$,
and $\mu = \mu_0 + \mu_1$ includes first-order corrections [Littlejohn'81]:

$$
\mu = \frac{(\mathbf{v}_\perp - \mathbf{v}_d)^2}{2B} - \frac{\mu_0 v_\parallel}{2B}[\hat{\mathbf{b}} \cdot \nabla \times \hat{\mathbf{b}} - 2(\hat{\mathbf{a}} \cdot \nabla \hat{\mathbf{b}}) \cdot \hat{\mathbf{c}}]
$$

$\mathbf{v}_d$ is magnetic gradient and curvature drift velocity, $\hat{\mathbf{c}} = \mathbf{v}_\perp / v_\perp$,
$\hat{\mathbf{a}} = \hat{\mathbf{b}} \times \hat{\mathbf{c}}$

GAE and CAE modes observed in NSTX shot # 141398

Experimental measurements

[N. Crocker, IAEA 2012, EX/P6-02]

- Detailed measurements of GAE and CAE modes amplitudes and mode structure were obtained for H-mode plasma in NSTX shot 141398.
- The modes have been identified as CAE modes for frequencies f>600 kHz, and small toroidal mode numbers $|n| \leq 5$.
- The modes have been identified as GAEs for f<600 kHz, and $|n| \sim 6-8$ based on dispersion relations.

HYM simulations

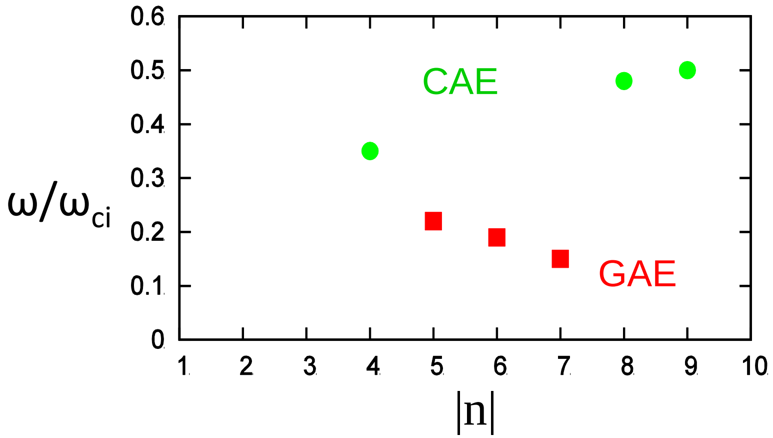

Frequency versus toroidal mode number for most unstable GAE (red) and CAE (green) modes, from HYM simulations for NSTX shot #141398. Frequency is normalized to ion cyclotron frequency at the axis f_{ci}=2.5MHz.

HYM simulations show that most unstable modes for n=5-7 are counter-rotating GAE modes, with shear Alfven wave polarization in the core, and comparable parallel and perpendicular components of perturbed magnetic field at the edge. The n=4 and n=8 and 9 modes are co-rotating CAE modes, which have been identified based on large compressional component of perturbed magnetic field.

CAE mode: effective potential well

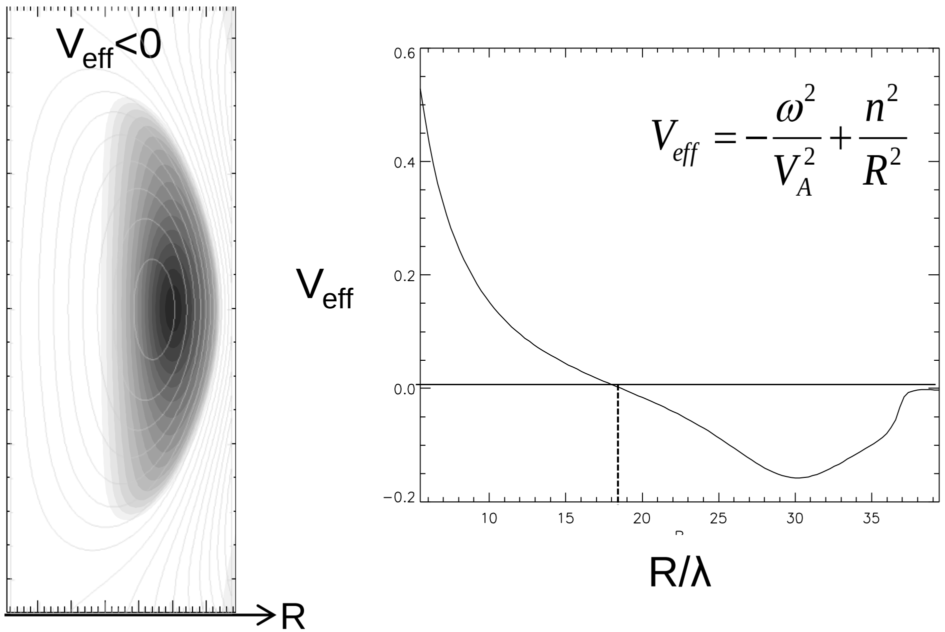

Approximate equation for CAE mode, assuming circular cross-section, and neglecting beam effects and coupling to SAW:

$$\frac{\partial^2 \delta B_{\|}}{\partial r^2} = V_{eff}\, \delta B_{\|}$$

$$V_{eff} = -\frac{\omega^2}{V_A^2} + \frac{n^2}{R^2} + \frac{m^2}{r^2}$$

Contour plot and radial profile of the effective potential V_{eff} for n=4 CAE mode with $\omega=0.35\omega_{ci0}$. Mode can exist for $V_{eff} < 0$ with radial extent: 18<R<37 (major radius is normalized to ion skin depth λ=3.93cm).

CAE vs GAE mode structure

n=4, CAE

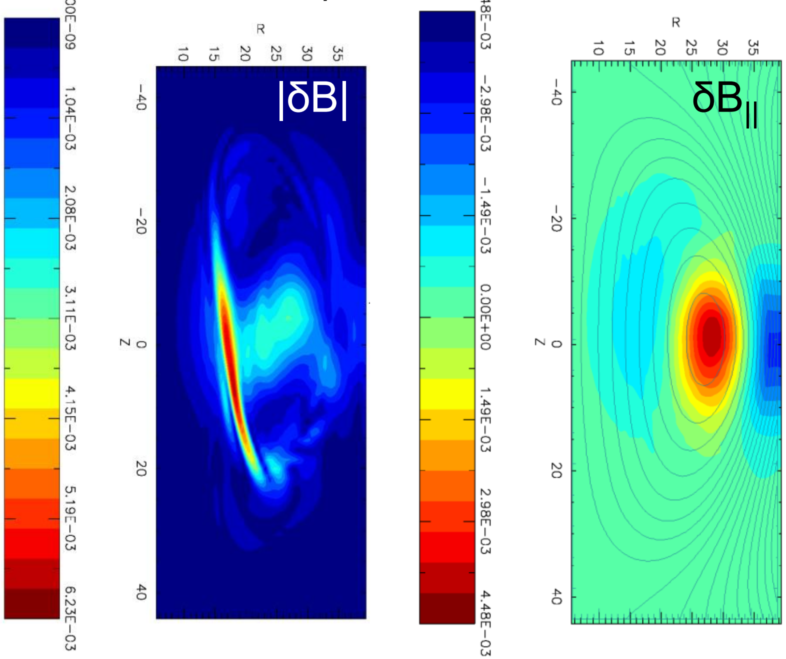

Contour plots of $|\delta B|$ and parallel components of magnetic field perturbation from HYM simulations of n=4 CAE mode.

n=6, GAE

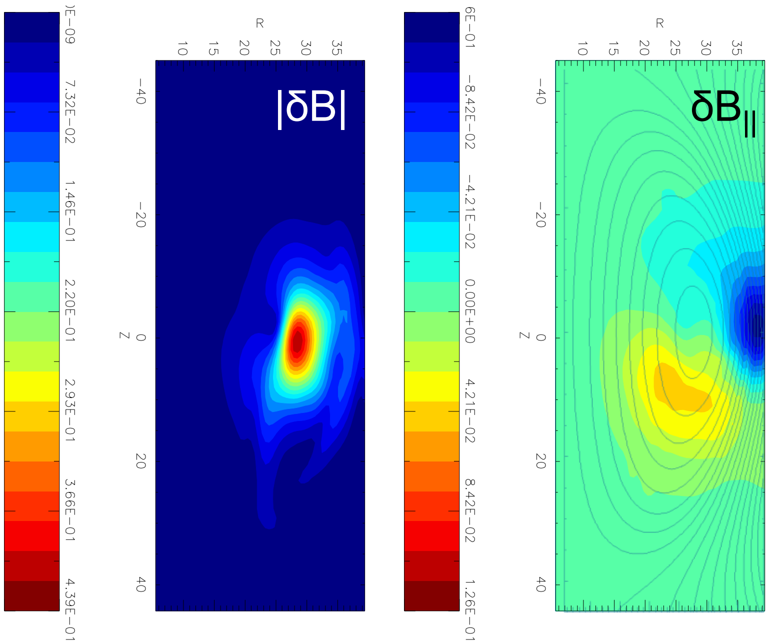

Contour plots of $|\delta B|$ and parallel components of magnetic field perturbation from HYM simulations of n=6 GAE mode; $\delta B_{||} < 0.3\,|\delta B|$.

For CAEs, $\delta B_{||}$ is significantly larger than $\delta B_{\perp}$ everywhere including the edge, whereas for GAEs, $\delta B_{||}$ is comparable to $\delta B_{\perp}$ only at the edge.

CAE mode couples with kinetic Alfven wave (KAW)

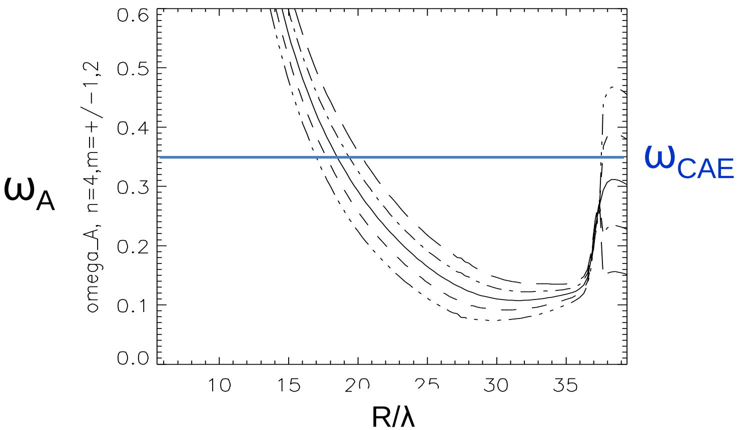

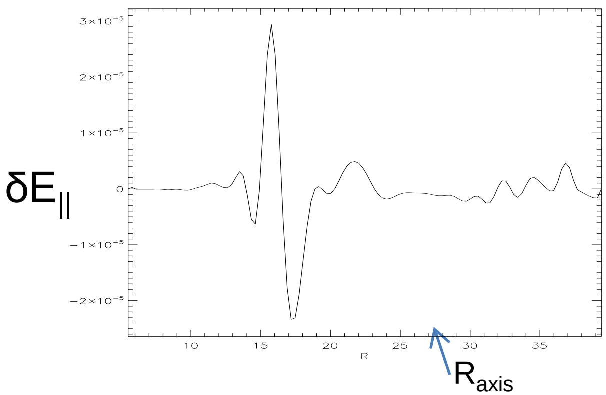

Radial profiles of Alfven continuum and $\delta E_{||}$. Radial width of KAW is comparable to beam ions Larmor radius.

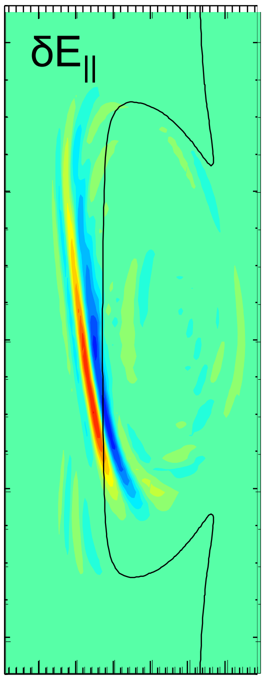

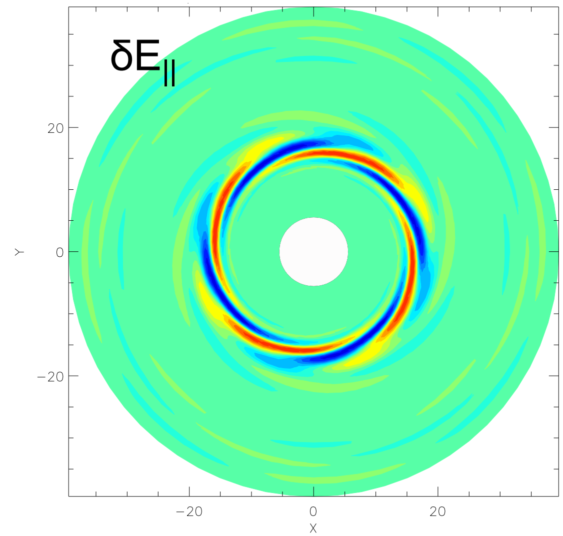

Poloidal and equatorial plane contour plots of $\delta E_{||}$, solid line is contour of $\omega_A(Z,R) = \omega_{CAE}$, where $\omega_A(Z,R) = V_A n/R$.

KAW can have strong effect on electron transport due to finite $\delta E_{||}$.

CAE structure: compressional vs shear components

$\delta B_{||}$

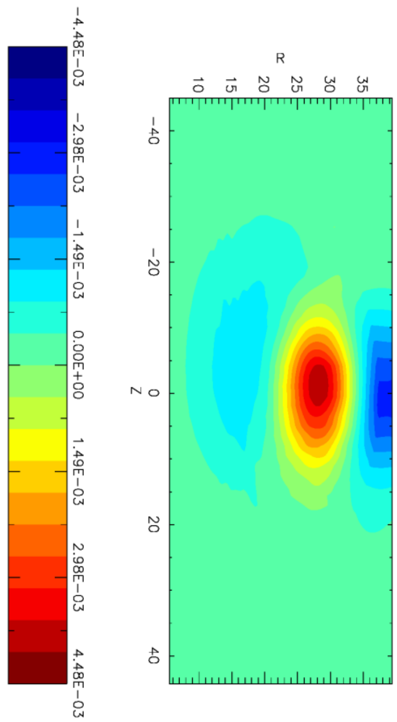

$|\delta B_{\perp}|$

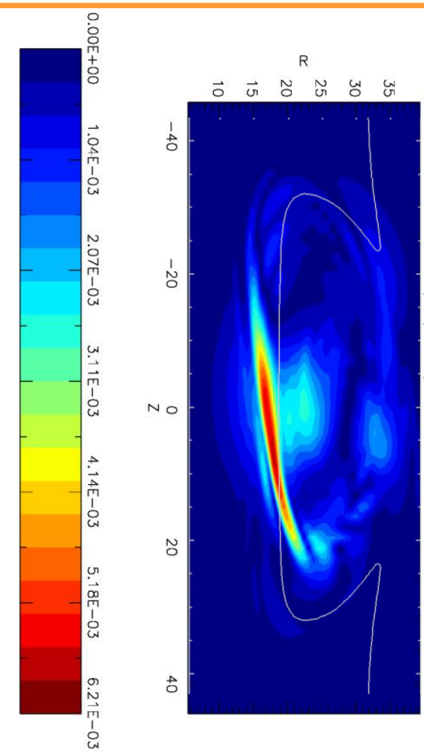

KAW structure is tilted relative to equilibrium magnetic field because $k_{||}$ is in the direction of the beam velocity, and $k_{\perp}$ directed towards high-density side with $k_{\perp} >> k_{||}$. This results in a mode structure which is not symmetric relative to mid-plane.

CAE structure: compressional vs shear components

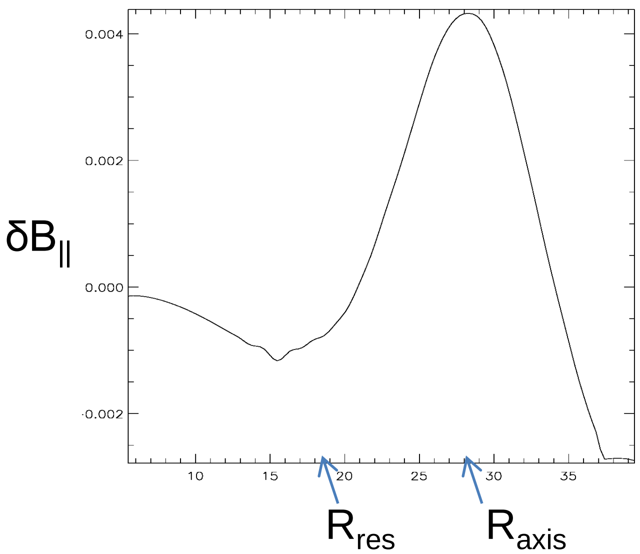

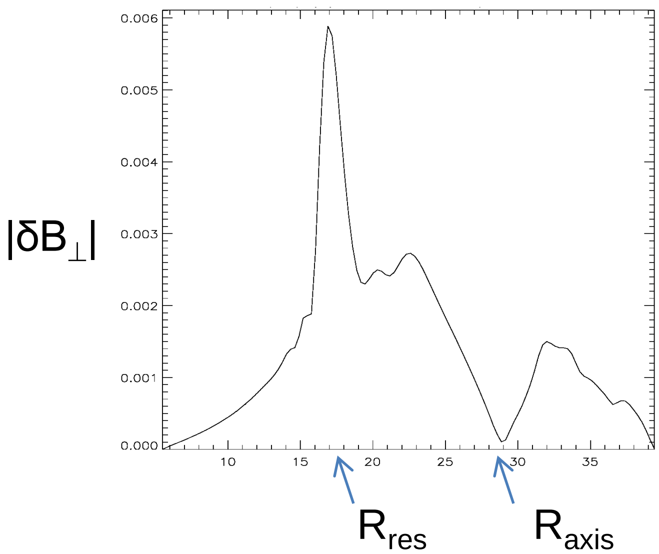

Near magnetic axis $\delta B_{||} >> \delta B_{\perp}$, at the edge $\delta B_{||}/3 \sim \delta B_{\perp}$.
At the KAW resonance location, $\delta B_{||} << \delta B_{\perp}$, and the amplitude of KAW is larger than the amplitude of driving CAE mode (major radius is normalized to ion skin depth λ=3.93cm).

Mode structure: compressional vs shear components

$\delta B_{||}$

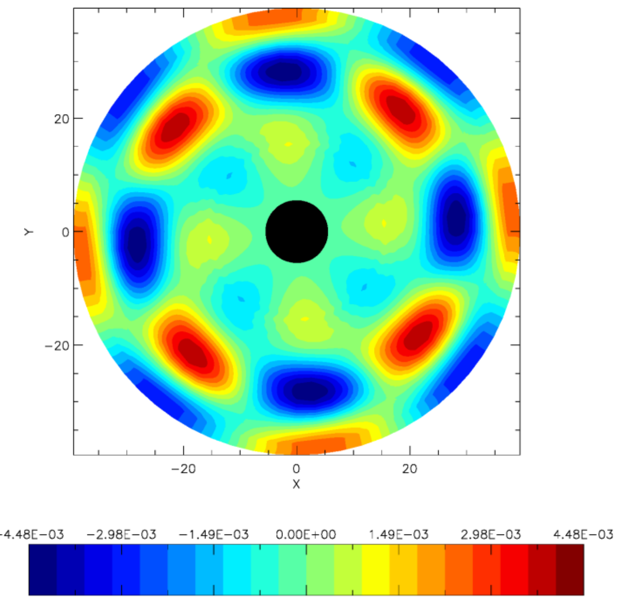

δB_z

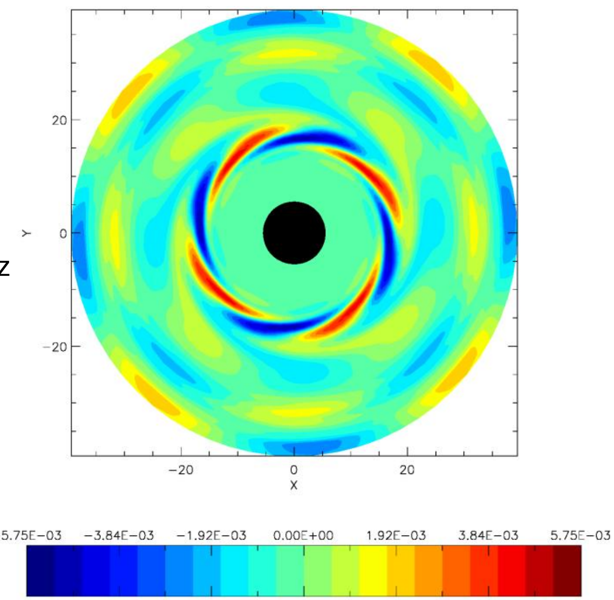

KAW structure is tilted relative to equilibrium magnetic field because $k_{||}$ is in the direction of the beam velocity, and $k_{\perp}$ directed towards high-density side with $k_{\perp} >> k_{||}$.

KAW structure

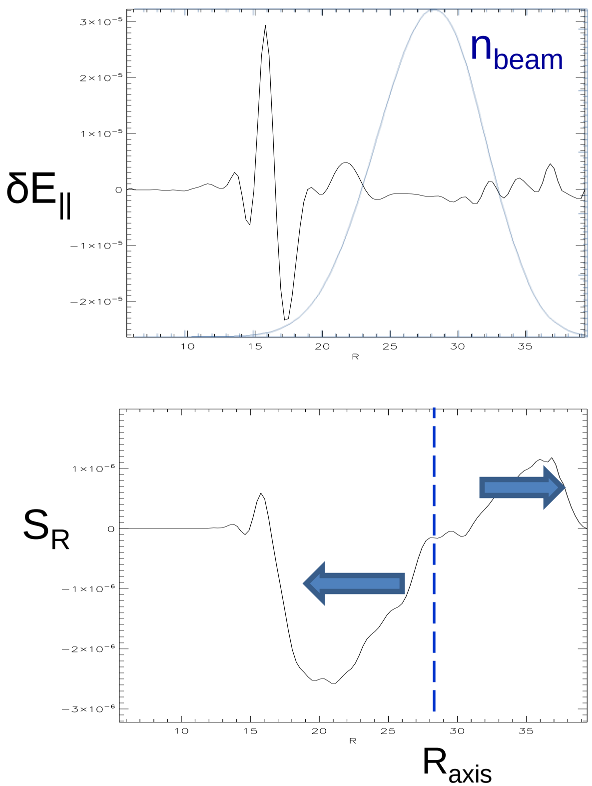

(a) Radial profiles of $\delta E_{||}$ and beam ion density; (b) Radial component of Poynting vector **S**=<**E**x**B**>.

- Resonance with KAW is located at the edge of CAE well, and just inside beam ion density profile.
- Resonant mode polarization is consistent with KAW mode, ie $\delta B_Z >> \delta B_R$, $\delta B_{||}$ and $\delta V_Z >> \delta V_R$, $\delta V_{||}$ with $\delta V_Z \sim -\delta B_Z$.
- Radial width of KAW is comparable to beam ions Larmor radius, $k_\perp \rho_{beam} \leq 1$.
- Energy flux is directed away from magnetic axis. Energy flux from the axis and dissipation at the resonant location can have direct effect on temperature profile.

n=8 co-rotating CAE mode: effective potential well

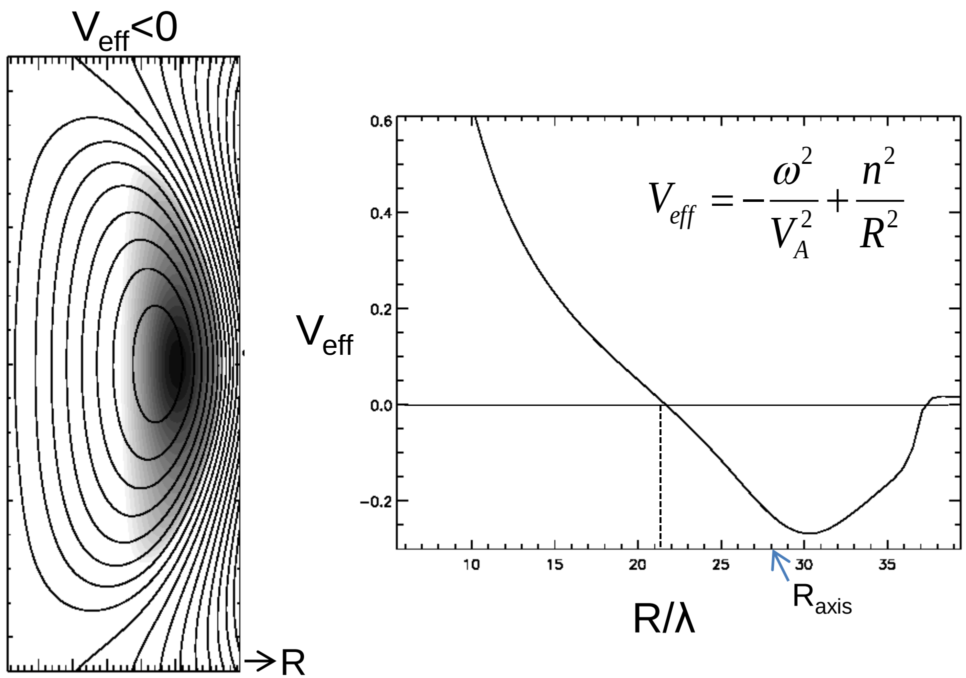

$$V_{eff} = -\frac{\omega^2}{V_A^2} + \frac{n^2}{R^2}$$

Effective potential well for n=8 mode is narrower and deeper than V_{eff} for n=4 resulting in more localized CAE mode with larger frequency.

HYM simulations show unstable n=8 mode with $\omega=0.48\omega_{ci0}$ and $\gamma=0.004\omega_{ci0}$.

Contour plot and radial profile of the effective potential V_{eff} for n=8 CAE mode with $\omega=0.48\omega_{ci0}$. Mode can exist for $V_{eff} < 0$ with radial extent: 22<R<37 (major radius is normalized to ion skin depth λ=3.93cm).

High-n CAE modes also show coupling to KAW

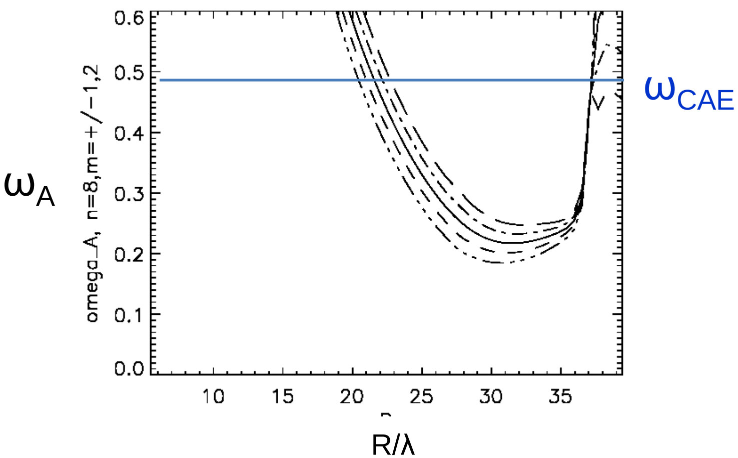

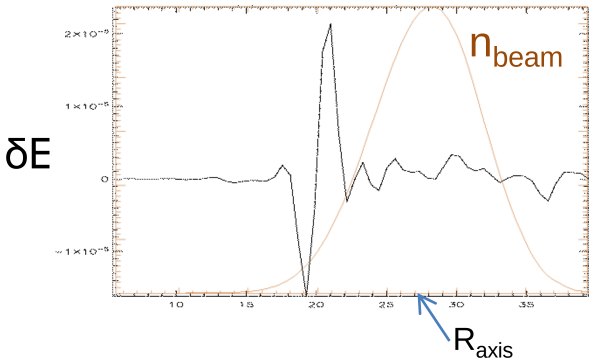

Radial profiles of Alfven continuum and $\delta E_{||}$. Radial width of KAW is comparable to beam ions Larmor radius.

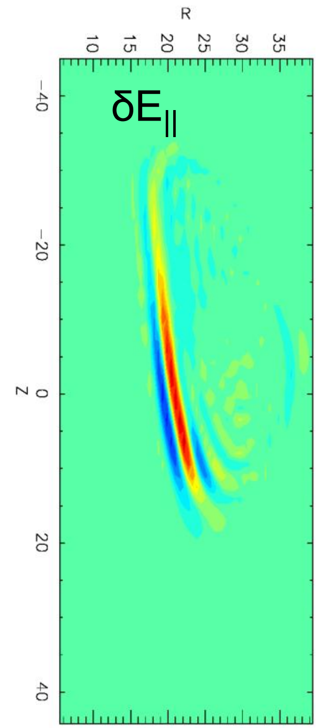

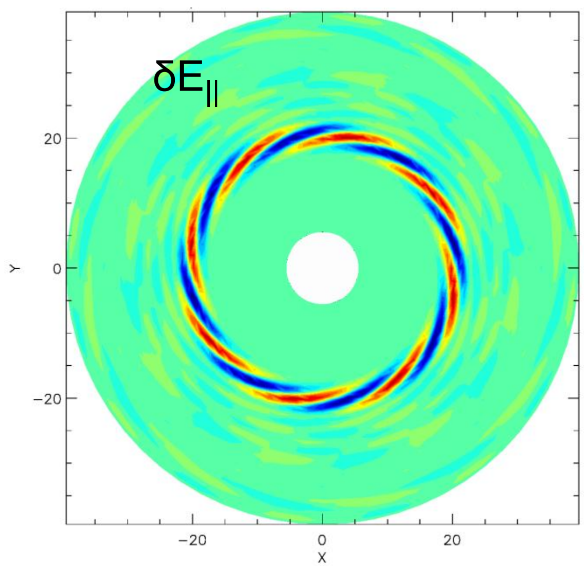

Poloidal and equatorial plane contour plots of $\delta E_{||}$, solid line is contour of $\omega_A(Z,R) = \omega_{CAE}$, where $\omega_A(Z,R) = V_A\, n/R$.

KAW can have strong effect on electron transport due to finite $\delta E_{||}$.

n=8 co-rotating CAE: mode structure

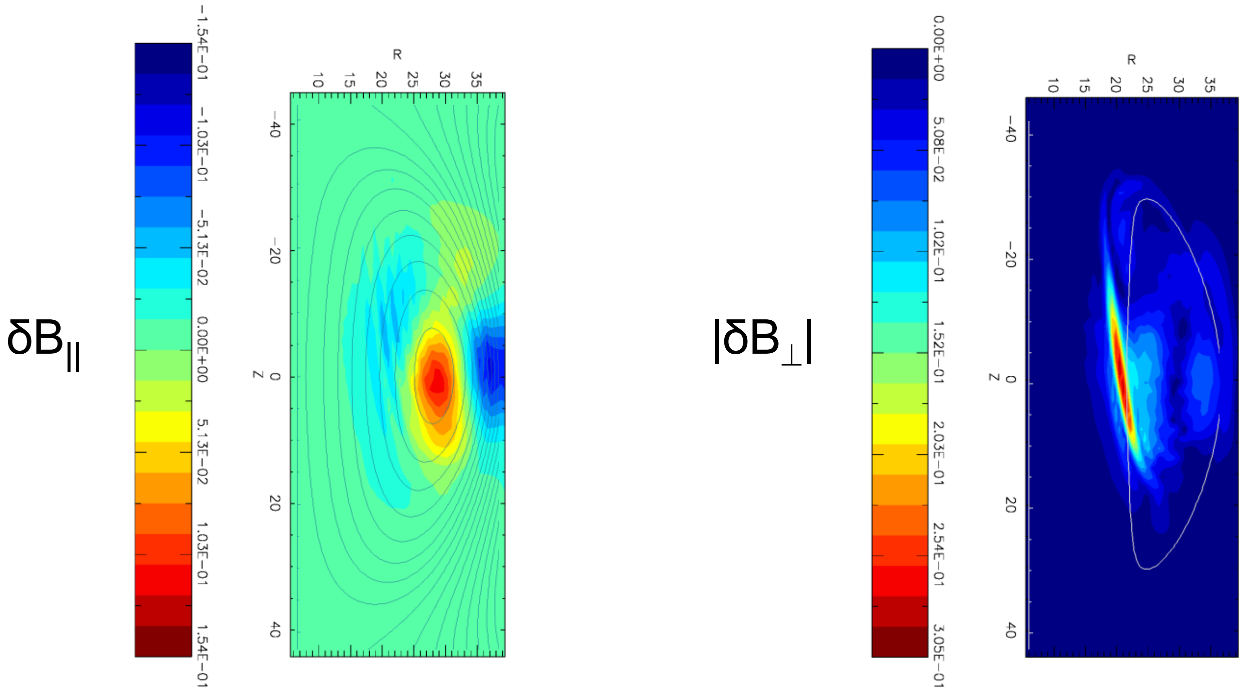

Higher-n co-rotating CAEs also show resonant coupling to KAW. CAE mode peaks near magnetic axis, where $\delta B_{||} >> \delta B_{\perp}$, KAW is located at the resonance (solid contour line of ω_A (Z,R)=ω_{CAE}) on HFS. KAW amplitude is double of maximum CAE amplitude.

Resonant particle plots, n=8 co-rotating CAE

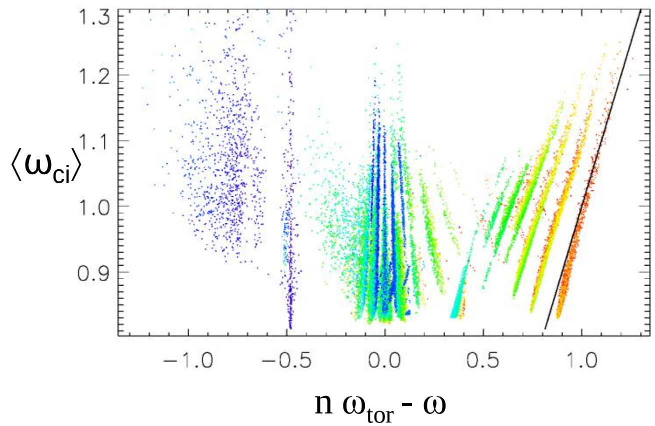

Resonant particles shown with orbit-averaged cyclotron and toroidal frequencies, both normalized to the ion cyclotron frequency at the axis, ω_{ci0}. From simulations of the n=8 co-rotating CAE mode with $\omega=0.48\omega_{ci}$. Particle colour corresponds to different energies: from E=0 (purple) to E=90keV (red).

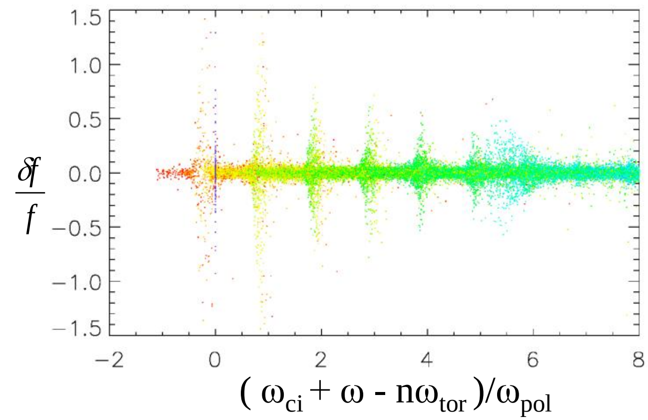

Particle weight vs anomalous cyclotron resonant condition: $\omega + \langle\omega_{ci}\rangle - n\omega_{tor} + k\omega_{pol} = 0$, where n=8, and k=0,±1,±2,… Poloidal frequency is small compared to other terms in the resonant condition, $\omega_{pol} \sim 0.08\ \omega_{ci0}$, resulting in the fine splitting of resonances.

- Two groups of resonant particles, one group which satisfy condition: $\omega - k_{||}v_{||} = 0$, and another which satisfy Doppler-shifted cyclotron resonant condition: $|\omega| + \omega_{ci} - |k_{||}v_{||}| = 0$.

- In contrast to unstable counter-rotating GAE modes, the Doppler shift is larger than the orbit-averaged cyclotron frequency for the large-n CAE modes (anomalous cyclotron resonance).

Location of resonant particles in phase-space

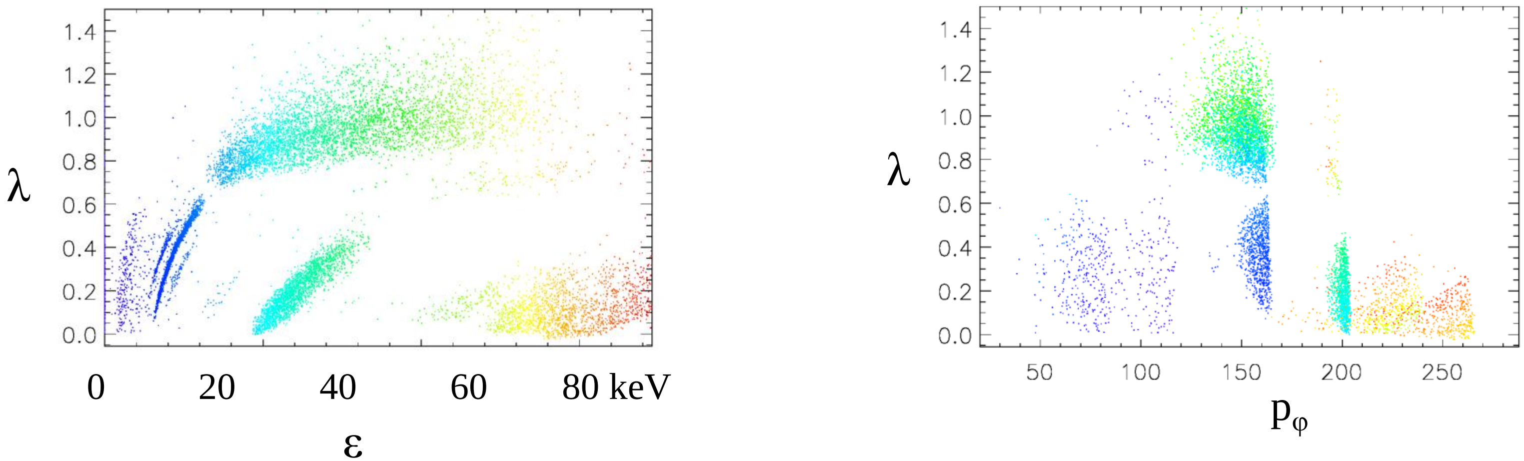

Location of resonant particles in phase space, (a) $\lambda=\mu B_0/\varepsilon$ vs energy, and (b) λ vs toroidal angular momentum $p_\varphi = Rv_\varphi - \psi$. From HYM simulations for NSTX shot #141398, $\omega=0.48\omega_{ci0}$, $\gamma=0.004\omega_{ci0}$. Particle color corresponds to different energies: from E=0 (purple) to E=90keV (red).

Location of resonant particles in phase-space

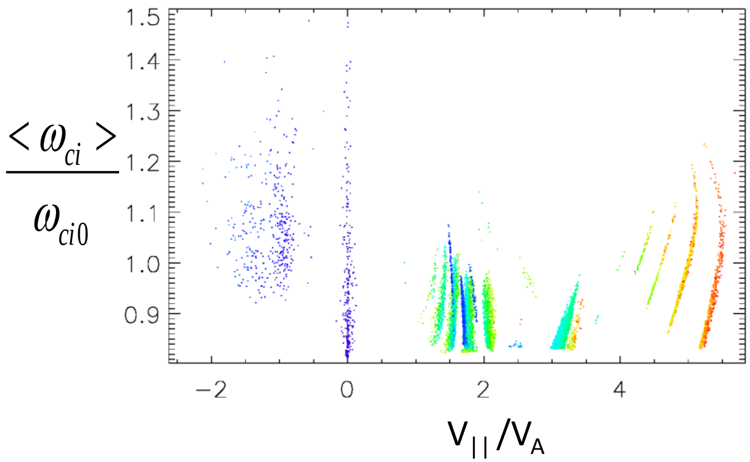

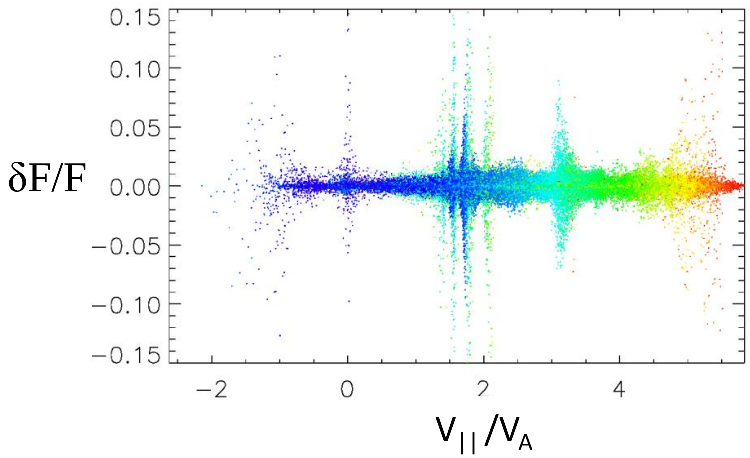

Location of resonant particles in phase space, (a) orbit-averaged cyclotron frequency vs orbit-averaged parallel velocity for resonant particles; (b) particle weight w ~ δF/F vs orbit-averaged parallel velocity for all simulations particles. From HYM simulations for NSTX shot #141398, $\omega=0.48\omega_{ci0}$, $\gamma=0.004\omega_{ci0}$. Particle color corresponds to different energies: from E=0 (purple) to E=90keV (red).

Conclusions

- Excitation of CAE modes have been studied for H-mode NSTX discharges. Equilibrium profiles and plasma parameters have been chosen to match the NSTX discharge profiles, using TRANSP.
- For CAEs, compressional magnetic field component is much larger than perpendicular component in the core.
- All unstable CAE modes are coupled with KAW on the HFS. Resonance with KAW is located at the edge of CAE well, and just inside beam ion density profile. Radial width of KAW is comparable to beam ion Larmor radius.
- Energy flux from the CAE to KAW and dissipation at the resonant location can have direct effect on temperature profile.
- For high-n co-rotating CAEs, two groups of resonant particles have been found, one group which satisfy condition: $\omega - k_{||}v_{||} = 0$, and another which satisfy the anomalous Doppler-shifted cyclotron resonant condition.